A Spectral BSSRDF for Shading Human Skin

Craig Donner and Henrik Wann Jensen[†]

Universtiy of California at San Diego, La Jolla, CA, USA

Abstract

We present a novel spectral shading model for human skin. Our model accounts for both subsurface and surface scattering, and uses only four parameters to simulate the interaction of light with human skin. The four parameters control the amount of oil, melanin and hemoglobin in the skin, which makes it possible to match specific skin types. Using these parameters we generate custom wavelength dependent diffusion profiles for a two-layer skin model that account for subsurface scattering within the skin. These diffusion profiles are computed using convolved diffusion multipoles, enabling an accurate and rapid simulation of the subsurface scattering of light within skin. We combine the subsurface scattering simulation with a Torrance-Sparrow BRDF model to simulate the interaction of light with an oily layer at the surface of the skin. Our results demonstrate that this four parameter model makes it possible to simulate the range of natural appearance of human skin including African, Asian, and Caucasian skin types.

Categories and Subject Descriptors (according to ACM CCS): I.3.7 [Computer Graphics]: Color, shading, shadowing, and texture

1 Introduction

Simulating the appearance of human skin is a challenging problem due to the complex structure of the skin. Furthermore, even small variations in color and shade significantly influence the perception of skin, as they convey information about a person's health, ethnicity, and physiological state. A physically accurate shading model that takes into account the full spectral interactions of light with tissue is essential for realistic renderings of human skin.

Light scattering in skin is dominated by subsurface scattering, which was first recognized in computer graphics by Hanrahan and Krueger [HK93]. They developed a BRDF model for skin that accounted for single scattering of light plus a diffuse term. Stam [Sta01] further enhanced this model by simulating multiple scattering of light. Marschner et al. [MWL*99] measured isotropic BRDFs of human skin and used these for rendering. These BRDF techniques, however, assume that light both enters and exits the skin at a single point, and they cannot simulate the softness and the color bleeding effects that are characteristic of translucent materials such as skin [JMLH01].

Debevec et al. [DHT*00] measured the reflectance field of human faces, allowing for rendering of skin under varying illumination conditions with excellent results. Jensen and Buhler [JB02], Hery [Her03] and Weyrich et al. [WMP*06] have investigated methods to measure the surface and subsurface properties of human faces. While these techniques can be used to reproduce measured data accurately, there is no clear way to modify model parameters arbitrarily to generate a desired appearance.

Tsumura et al. [TM99, TOS*03] developed an image-based technique to recover and subsequently model the concentrations of melanin and hemoglobin in skin. Their method makes the assumption that melanin and blood have completely independent effects on skin color, which has been shown to not be the case [SzZKB04]. Also, their technique is limited to specific camera-light combinations.

Jensen et al. [JMLH01] developed a BSSRDF model for simulating subsurface scattering within translucent materials, and showed how their model captures both the softness and the color bleeding characteristics of human skin. They also measured optical parameters for skin assuming that skin is a homogenenous semi-infinite medium. Donner and Jensen [DJ05] later developed a BSSRDF model for thin or layered materials. They demonstrated how their technique

---

[†] Email:{cdonner, henrik}@graphics.ucsd.edu

could to be used to simulate light scattering within a three layer model of human skin based on measurements of the scattering properties of the individual layers. While these diffusion methods can produce realistic renderings of human skin, it is again unclear how to set the parameters for the model other than relying on measured values or ad hoc parameters.

Krishnaswamy and Baranoski [KB04] developed the BioSpec model for simulating light interaction with human skin. The BioSpec model is based on a detailed model of human skin that uses physically obtained biological parameters to simulate the transport of light through the different layers of skin. It models the spectral scattering and absorption properties of the skin, using brute-force Monte Carlo ray tracing to simulate scattering within the skin model. This makes the BioSpec model significantly more costly than diffusion style methods. In addition, there is no clear way to accelerate the BioSpec model using diffusion-based techniques, as it does not compute radially symmetric profiles. The model is quite complex having almost two dozen input parameters, and the interactions between parameters, as well their individual and combined effects on overall appearance, is complicated. It is also unclear how to determine these parameters for a desired skin type, making it difficult to use the BioSpec model for simulating the appearance of human skin.

In this paper, we present a practical physically-based spectral shading model for rendering human skin. The model accounts for subsurface scattering within the skin and surface reflection of the oily surface. It is controlled by four physically meaningful parameters that control the amount of melanin, hemoglobin, and the oiliness of the skin. We use the multipole method for layered materials [DJ05] to efficiently calculate spectral diffusion profiles for a two-layer model of the skin. These diffusion profiles are used during rendering to simulate the subsurface scattering of light within the skin. To account for the reflection of light by the oily skin surface we use a Torrance-Sparrow model. We demonstrate our model by simulating different skin types (African, Asian and Caucasian), and show that it reproduces the spectral reflectance behavior characteristics of human skin.

2   The structure of skin and its interaction with light

The physical structure and chemical makeup of skin is a well studied topic in various scientific fields. Skin is known to have a distinct layered structure, with smaller-scale structures (hair follicles, wrinkles, sweat glands, capillary veins, etc.), all of which have some effect on appearance [INN05].

2.1   Absorption of light

The most striking feature of skin is its color, which is determined by absorbing chromophores distributed in the different layers. The most prominent chromophores that affect skin appearance are hemoglobin and melanin [AP81]. Hemoglobin is responsible for carrying oxygen throughout the body, and
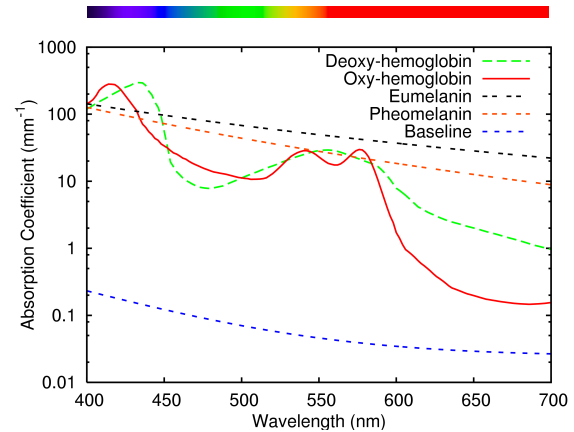

Figure 1: Spectral absorption coefficients of hemoglobin, melanins, and baseline skin absorption.

is the primary constituent of red blood cells. It comes in both oxygenated and deoxygenated forms, each with a slightly different properties. The absorption spectra of both oxy- and deoxy- hemoglobin are shown in Figure 1. Note the characteristic peaks in oxy-hemoglobin at 542nm and 547nm.

The other chromophore, melanin, is not actually a pure substance, but is composed of different polymers, and varies in color from light yellow to very dark brown or black [AAB*02]. Lighter melanin is composed mostly of *pheomelanin*, while the darker type is generally *eumelanin*. Different concentrations of these basic molecular building blocks are believed to produce the various pigmentations of skin and hair seen in the natural world. Both melanins have a characteristicly broad and smooth absorption band, with highest absorption in the UV range, decaying as wavelength increases (see Figure 1). This property likely makes them good safeguards against solar radiation. Recent work suggests that the the *type*, rather than total concentration, of melanin is the primary factor in skin coloring [AAB*02]. Although the most significant absorber in the darkest skin is eumelanin, in somewhat lighter skin colors (e.g. Asian skin), there is a wide range of concentrations of the different types of melanin [AHC*01, AAB*02, IW06, WKK*06]. The particular type distribution varies by individual, even within a single ethnic group.

There are small concentrations of other chromophores carried in the blood, such as bilirubin and beta-carotene, but their visible contribution in healthy skin is negligible [AP81, MM02]. The other structures in skin, such as internal cellular structures and organelles, also play some small part in absorbing light.

2.2   Scattering of light

Besides having a complex absorption spectrum, skin is also a highly scattering material. This is primarily due to high frequency changes in index of refraction within the small-scale

structures of the skin, and in particular due to collagen and elastin fibrils that run beneath the surface [AP81]. The distribution of these fibrils generally decreases in concentration with depth [MM02]. Chromophores also play a small role in the scattering of light within the skin.

2.3 Skin layers

Skin has a definite layered structure. The highest level of the skin is the *stratum corneum*, and is quite thin, highly scattering, but absorbs almost no light. The layers below the stratum corneum are associated with the epidermis, and this is where most of the melanin in skin is found [AP81]. Below the epidermal layers is the dermis, where the vascular network carrying nutrients to tissues via the blood is found. The dermal layers contain most of the blood in healthy skin. Even deeper below the dermis is the subcutaneous tissue, such as fat, but it has little effect on visible appearance [MM02].

The skin also secretes an oily substance, the sebum, which contributes to the direct surface reflection of light [NL01]. Light that is not reflected off the surface scatters amongst the tissues of the skin, where it is either absorbed by chromophores, or scattered out.

3 A two-layer model for human skin

In this section we present a new practical appearance model for skin. We draw on some of the ideas behind both the BioSpec [KB04] and diffusion-based models [JMLH01, DJ05], but focus on developing a model with a minimal set of parameters most important for skin appearance. The goal is a model that is realistic, but also intuitive and simple to control. We use four parameters to control the oiliness, hemoglobin concentration, melanin concentration, and a blend factor between the different types of melanin. Each of these is discussed in more detail below.

Our shading model consists of three terms

- a surface reflection term for directly reflected light due to oil,
- a spectral subsurface scattering term for light transported through the skin,
- and a texturing term using a surface albedo map.

The skin color produced by our model is given as the sum of the surface reflection and the texture-modulated subsurface scattering terms.

3.1 Surface reflection

Direct reflection is due mostly to oil on the surface of the skin, as well as the skin's intrinsic roughness. We also include scattering from the stratum corneum in this term, as this thin highly scattering layer does not significantly blur the incident light.

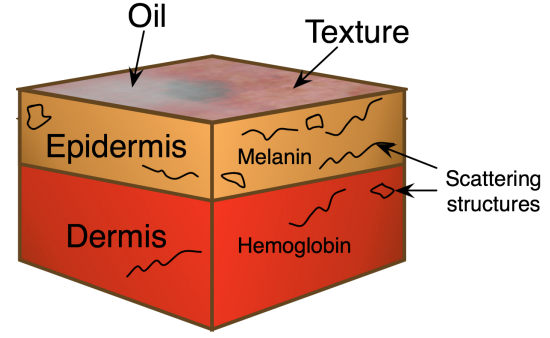We model direct reflection with the Torrance-Sparrow microfacet BRDF [TS67], which has been previously shown to

Figure 2: *Two layer model of skin.*

give good visual results when fitting specular highlights from skin [DHT*00, WMP*06]. The BRDF is

$$f_{r,TS} = \rho_s \frac{F(x, \vec{\omega}_o, \vec{\omega}_i) \cdot D(x, \vec{\omega}_o, \vec{\omega}_i, \sigma) \cdot G(x, \vec{\omega}_o, \vec{\omega}_i)}{4(\vec{\omega}_i \cdot \vec{n})(\vec{\omega}_o \cdot \vec{n})} \quad (1)$$

where $\vec{\omega}_i$ and $\vec{\omega}_o$ are the incoming and outgoing lighting directions, F is the Fresnel reflectance, G is the geometry term, and D is the Beckmann microfacet distribution [CT82]. The parameter σ controls the RMS slope of the microfacets, and is often referred to as the "roughness" parameter. We have found that values for σ in the range $0.2 - 0.4$ give good results for skin, and we use $\sigma = 0.35$ for all our results. Rather than changes σ, we use ρ_s to control the oiliness of the skin surface.

Similar to [DJ05], we calculate an average diffuse reflectance by integrating the BRDF over the outgoing hemisphere

$$\rho_{dr}(x, \vec{\omega}_i) = \int_{2\pi} f_{r,TS}(r, \vec{\omega}_o, \vec{\omega}_i)(\vec{\omega}_i \cdot \vec{n}) d\vec{\omega}_o. \quad (2)$$

Any light that is not reflected is assumed to transmit into the skin, thus the subsurface scattering term is modulated by $(1 - \rho_{dr})$. This helps ensure conservation of energy. In most cases, less than 10% of the incident light is reflected at the surface, making this a good approximation of the actual light distribution.

3.2 Subsurface scattering

We simulate subsurface scattering in a two layered model of the skin (see Figure 2). Many other authors have found a two-layer model to be sufficient for skin [TG79, vJSS89, SSAS97, TOS*03], though existing models range from a single layer [JMLH01] to seven layers [MM02]. Closer analysis of the properties of different layers of skin, however, shows that there is little variation in their optical properties [MM02], and that a two-layer separation into an epidermal and dermal layer is adequate [AP81].

To model the scattering and absorption of light in the skin, we have developed a two layer skin model, representing the skin as an epidermis and dermis. We use the multipole dif-

fusion model [DJ05] to compute spectral diffusion profiles that can be directly used for rendering. The multipole accurately predicts the diffuse reflectance from layered translucent materials, comparing well both to measured data and other existing simulation techniques [DJ06]. To use the multipole it is necessary to know the optical properties of each layer, namely their absorption and reduced scattering coefficients σ_a and σ_s'. For skin, these coefficients are determined by the chemical composition and structure of each layer, and we describe those elements in the following sections.

3.3 Absorption by the epidermis

The primary chromophore in the upper areas of skin is melanin. As mentioned previously, melanin is not a pure substance, but rather a complex combination of different molecules. Both the amount and type of melanin present in the skin are thought to contribute to overall color. The two extreme types of melanin are brown-black eumelanin, and yellowish-red pheomelanin.

Because both types of melanin have fairly featureless absorption spectra, increasing with shorter wavelength, their absorption spectra are approximated well by simple power laws [SJT95]

$$\sigma_a^{em}(\lambda) = 6.6 \times 10^{10} \times \lambda^{-3.33} \quad mm^{-1} \tag{3}$$

$$\sigma_a^{pm}(\lambda) = 2.9 \times 10^{14} \times \lambda^{-4.75} \quad mm^{-1} \tag{4}$$

where λ is the wavelength of light in nanometers, σ_a^{em} is the spectral absorption coefficient of eumelanin, and σ_a^{pm} of pheomelanin. Equation 3 fits data from [JM91], while Equation 4 is our empirical fit to data from data in [SS98]. Baseline skin absorption from other small scale tissues in the epidermis (organells, cell membranes, fibrils, etc.) is approximated by [Jac98]

$$\sigma_a^{baseline}(\lambda) = 0.0244 + 8.53 e^{-(\lambda-154)/66.2} \quad mm^{-1} \tag{5}$$

We assume that both melanin and the small scale tissues are uniformly distributed throughout the epidermis. We define the total spectral absorption of the epidermis to be a combination of absorption from both

$$\sigma_a^{epi}(\lambda) = C_m \left(\beta_m \sigma_a^{em}(\lambda) + (1 - \beta_m)\sigma_a^{pm}(\lambda) \right) \\ + (1 - C_m)\sigma_a^{baseline} \tag{6}$$

where C_m is the total volume fraction of melanin in the epidermis, and β_m controls the amount of eumelanin relative to pheomelanin, and allow for a light tan or yellowish appearance. Low values of β_m give primarily pheomelanin, while values of β_m near 1 give primarily eumelanin, and give skin a brown or black appearance. Note that both kinds of melanin are found in various concentrations in most individuals, regardless of race, though it is generally thought that certain skin types are more likely to contain higher amounts of pheomelanin, such as Asian skin [HOD*05]. Darker skin types, such as African skin, contain higher total concentrations of melanin, mostly eumelanin.

Parameter	Description	Typical range
C_h	Hemoglobin fraction	$0.001 - 0.1$
C_m	Melanin fraction	$0 - 0.5$
β_m	Melanin type blend	$0 - 1$
ρ_s	Oiliness	$0 - 1$

Table 1: *Parameters to our model.*

3.4 Absorption in the dermis

The dermal layer approximates the deeper areas of skin that contain the vascular capillary network carrying blood. Here the primary chromophore is hemoglobin [SSAS97]. Hemoglobin exists in both an oxygenated and deoxygenated state within the dermis, each with a somewhat different absorption spectrum as shown in Figure 1. Again, we assume that hemoglobin is uniformly distributed in the dermis. We define the total spectral absorption of the dermis as a combination of absorption from hemoglobin and small scale structures

$$\sigma_a^{derm}(\lambda) = C_h \left(\gamma \sigma_a^{oxy}(\lambda) + (1 - \gamma) \sigma_a^{deoxy}(\lambda) \right) \\ + (1 - C_h)\sigma_a^{baseline} \tag{7}$$

where C_h is the fractional amount of hemoglobin in the dermis (usually about $0.1\% - 20\%$ depending on location and skin type), and γ is the blood oxygenation ratio between deoxy- and oxy-hemoglobin. γ varies only slightly over different skin types and body locations from about $0.6 - 0.8$ [ZBK01]. In our model we fix γ to be 0.75.

3.5 Scattering and thickness

The spectral scattering of light due to elastin and collagen fibrils, as well as other small-scale structures and chromophores in the skin, is approximated well by power laws that model a combination of Mie and Rayleigh theory [BGKT05]

$$\sigma_s'(\lambda) = 14.74\lambda^{-0.22} + 2.2 \times 10^{11} \times \lambda^{-4}. \tag{8}$$

The deeper regions of the skin are generally less scattering than the upper areas, as there is a lower concentration of scatterers [Jac96]. We assume that the reduced scattering coefficient is constant throughout each layer, but we scale the reduced scattering coefficient by 50% in the dermis, where the skin is more translucent.

We fix the thickness of the epidermal layer to 0.25*mm*, as chromophore pigmentation dominates the effects of changing thickness [SMPW03]. For simplicity, we also assume a constant index of refraction of 1.4 throughout the skin, as the actual index changes only slightly [MM02]. Since little light reaches subcutaneous tissue, we assume the dermis to be semi-infinitely thick.

The above equations generate spectral absorption and reduced scattering coefficients for the two skin layers. These become wavelength dependent inputs to the multipole model, which generates spectral diffusion profiles for each layer and
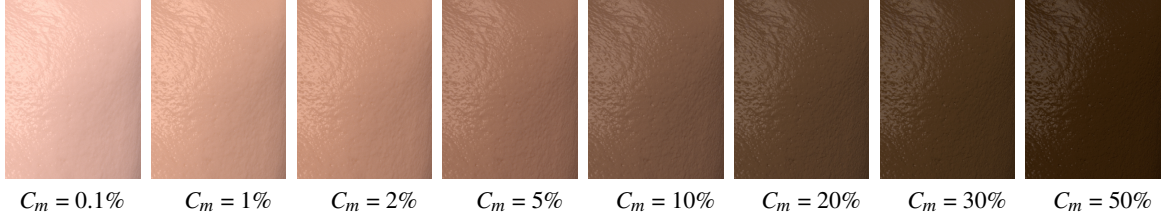
$C_m = 0.1\%$	$C_m = 1\%$	$C_m = 2\%$	$C_m = 5\%$	$C_m = 10\%$	$C_m = 20\%$	$C_m = 30\%$	$C_m = 50\%$

Figure 3: *Change in skin color of a skin patch as melanin volume fraction C_m is increased from 0.1% to 50%. Note the change in color from light Caucasian skin to dark African skin as the total amount melanin increases. The melanin blend β_m is fixed at 0.7, which is 70% eumelanin, and 30% pheomelanin. The hemoglobin fraction C_h is constant at 0.5%, and the oiliness ρ_s is 0.5.*

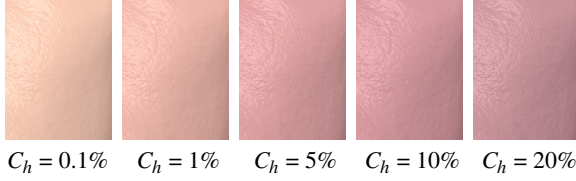| $C_h = 0.1\%$	$C_h = 1\%$	$C_h = 5\%$	$C_h = 10\%$	$C_h = 20\%$

Figure 4: *Change in skin color of a skin patch as the hemoglobin fraction C_h is increased from 0.1% to 20%. Less hemoglobin gives rise to a pale, translucent appearance to the skin, while more hemoglobin makes the skin look pink, and then purple. Total melanin fraction C_h is fixed at 1%, with β_m at 0.5. The oiliness ρ_s is 0.5.*
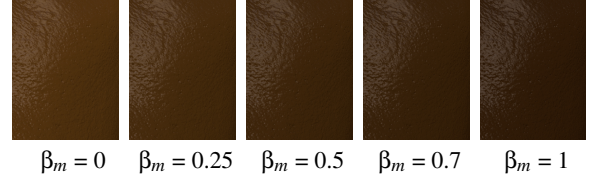

$\beta_m = 0$	$\beta_m = 0.25$	$\beta_m = 0.5$	$\beta_m = 0.7$	$\beta_m = 1$

Figure 5: *Change in skin color of a skin patch as the melanin blend β_m increases from 0 to 1. Lower values of β_m (more pheomelanin) give the skin a more yellowish appearance, while higher values (more eumelanin) give pure shades of tan and brown. The hemoglobin fraction C_h is constant at 0.1%, the total melanin volume fraction C_m is 50%, and the oiliness ρ_s is 0.5.*

convolves them together to provide a single, spectral diffusion profile for skin.

3.6 Texturing

An efficient way to locally modify the subsurface scattering term is to modulate it with an albedo texture. This includes fine scale details such as freckles, splotches, etc. Rather than requiring recalculation of diffusion profiles over the entire skin surface, we enable this local change directly with texture maps.

Since most textures include overall color data, they may include global melanin and hemoglobin pigments. These can be approximately removed by normalizing the texture [DJ05], or by subtracting out an assumed chromophore contribution. This is done by first finding the total diffuse reflectance

$$R_d = \int_0^\infty R(r) r \, dr \qquad (9)$$

where $R(r)$ is the multipole reflectance, calculated using assumed values of C_h, C_m, and β_m. Each pixel in the texture is then divided by this total diffuse reflectance rather than the texture average, leaving only local color variation. Removing global color from the texture in this way also provides an easy way to match existing images of skin, as the multiplication of the subsurface scattering term recovers the original texture color.

4 Implementation

Table 1 summarizes the four parameters to our model, with typical values. To use the model the user chooses values for each of the parameters C_m, β_m and C_h. These parameters, using Equations 3-8, directly give the spectral scattering and absorption coefficients of both the epidermis and dermis. We currently sample every $2nm$ from $400nm$ to $700nm$ to ensure accurate representation of the spectra, but such high-resolution sampling is not required. We have also tried converting these spectra to RGB absorption and reduced scattering coefficients, but this tends to overly smooth the effective spectra. The complex spectral interactions between the diffusion profiles of the layers are lost, leading to undesirable and unrealistic results. This finding is consistent with previous work [KB04].

Using the diffusion multipole, we calculate diffusion profiles for both layers using their spectral properties, and convolve them together to get a spectral diffusion profile for skin. During rendering, this profile is sampled using standard Monte Carlo techniques as described in [DJ05] to generate the subsurface scattering component. In our current implementation, the profile generation is done as a pre-process, and takes a few seconds. Conversion to RGB to generate images is done by first converting the calculated subsurface scattering color to XYZ and then RGB using the standard CIE $2°$ color matching functions, with the D65 illuminant. This resulting RGB value is scaled by the diffuse surface BRDF and albedo texture, and surface reflection is added as described in the
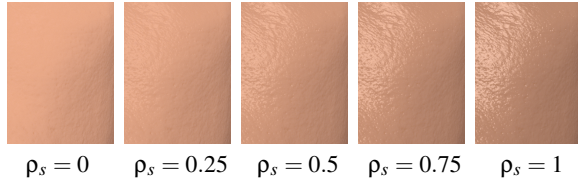
| $\rho_s = 0$ | $\rho_s = 0.25$ | $\rho_s = 0.5$ | $\rho_s = 0.75$ | $\rho_s = 1$ |

Figure 6: *Effect of changing ρ_s. Little or no oil leaves the skin looking featureless and diffuse, while increasing ρ_s adds specular detail to the surface, resulting in a more realistic appearance. Higher amounts of oil tend to desaturate the skin color, as more light is directly reflected at the skin's surface.*

previous sections using the parameter ρ_s. Overall rendering times are comparable to those of [JMLH01] and [DJ05], as the spectral sampling adds little overhead to the underlying algorithm.

5 Results

We have implemented the skin model in a Monte Carlo ray tracer capable of sampling spectral diffusion profiles. In the following, we examine how the four parameters of the model influence the appearance of rendered skin, and we show examples for different skin types. Unless explicitly stated, the images are of untextured skin. The rendering times for all images is below 10 minutes on a standard PC.

Figure 3 shows the effect of changing the melanin volume fraction C_m. The image shows a patch of skin on the right side of a face. Although only a single parameter is adjusted in this figure, a wide range of different skin types is simulated. From left to right, the changes in skin coloration reflect an increase in total melanin fraction from 0.1% to 50%. The leftmost images correspond to light Caucasian skin, while the rightmost images correspond to dark African skin. The middle images resemble tanned Caucasian or light Asian skin. The melanin blend β_m is held constant at 0.7, indicating 70% eumelanin and 30% pheomelanin, which gives these skin patches a characteristic beige/tan/brown appearance.

To illustrate the effect of changing hemoglobin volume fraction, Figure 4 shows the effect on skin color as C_h increases from 0.1% to 20% from left to right. Low values of C_h generate pale translucent skin, while higher values give pink and purple skin. Note that the skin does not become red, as in the case of a sunburn, as hemoglobin is only increasing in the dermis, and not the epidermis. Simulating this effect would require adding an additional hemoglobin fraction to the epidermis.

Next, in Figure 5, we show the effects of adjusting the melanin blend β_m from 0 to 1 from left to right. Lower values of β_m (higher pheomelanin content) give the skin a more yellowish appearance, which is common in dark Asian skin. Higher values of β_m (higher eumelanin content), make the skin a pure brown, consistent with African skin. Note that β_m
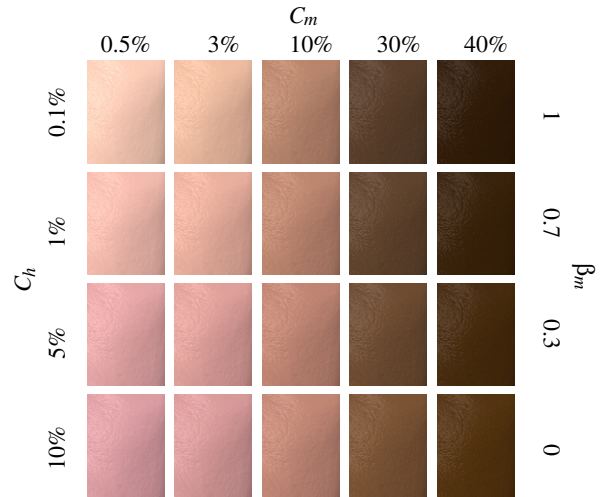

Figure 7: *Images showing the change in skin subsurface reflectance and color bleeding over the range of appearance produced by melanin, melanin blend, and hemoglobin change. The sweatiness/oiliness was kept constant at $\rho_s = 0.4$. Note that darker skin appears wetter because more of the light transmitted into the skin is absorbed, even if surface reflectance is the same compared to lighter skin. Also, the effects of higher blood concentration are less apparent in darker skin, as melanin absorption dominates. From top to bottom, the melanin blend β_m changes from 1 to 0.7, 0.3, and 0, and hemoglobin fraction C_h increases from 0.1% to 1%, 5%, and 10%. From left to right, the total melanin fraction increases from 0.1% to 0.5%, 3%, 20%, and 50%.*

does not have a significant effect on lightly pigmented skin (low values of C_m), since it has low amounts of total melanin.

Figure 6 shows the effects of adjusting the oiliness, ρ_s; the surface roughness σ is fixed at 0.35. Too little oil leaves the skin looking dry and diffuse, while too much gives the skin a wet and overly shiny appearance. In this figure, the amount of oil is kept constant over the surface of the skin, but it could easily be varied spatially with a parameter texture map, as the surface contribution is independent of the subsurface and texture components.

Figure 7 demonstrates the overall effects of changing only the three chromophore parameters of the model (C_m, C_h, and β_m). The parameters used are summarized in the figure captions. From left to right, melanin increases, and from top to bottom hemoglobin increases while the melanin blend changes decreases. Caucasian skin corresponds roughly to the upper left corner of the figure, with dark African skin in the upper right. Asian skin tends to fall near the middle of the figure, though there is the possibility for wide variation.

Using the four model parameters, it is simple to transition from the characteristics of one skin type to another by slightly
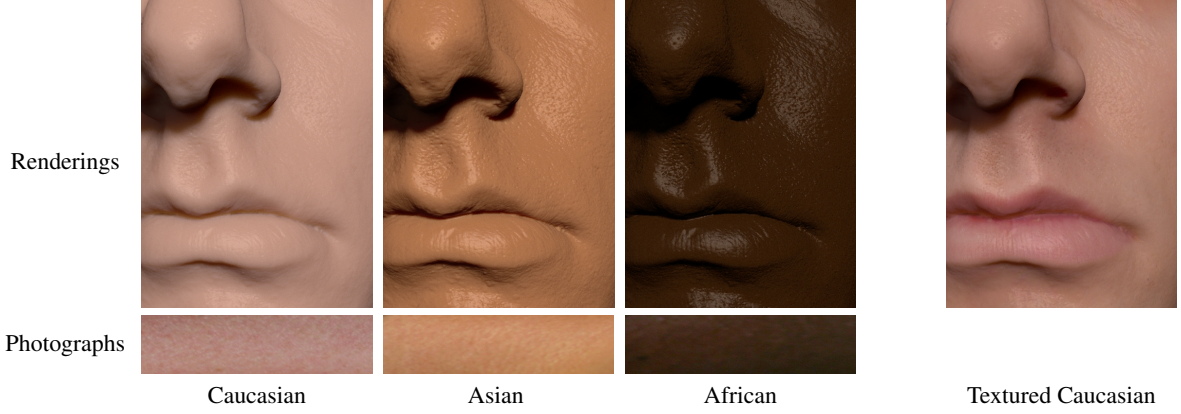
| | Caucasian | Asian | African | Textured Caucasian |

Renderings

Photographs

Figure 8: *Different skin types simulated with our model (top) compared to actual photographs of real skin samples (bottom). For Caucasian skin, $C_m = 0.5\%$, $\beta_m = 0.7$, $C_h = 0.5\%$, and $\rho_s = 0.3$. For Asian skin, $C_m = 15\%$, $\beta_m = 0$, $C_h = 1\%$, and $\rho_s = 0.3$. For African skin, $C_m = 50\%$, $\beta_m = 0.7$, $C_h = 5\%$, and $\rho_s = 0.3$. The far right image applies an albedo texture to the Caucasian skin.*
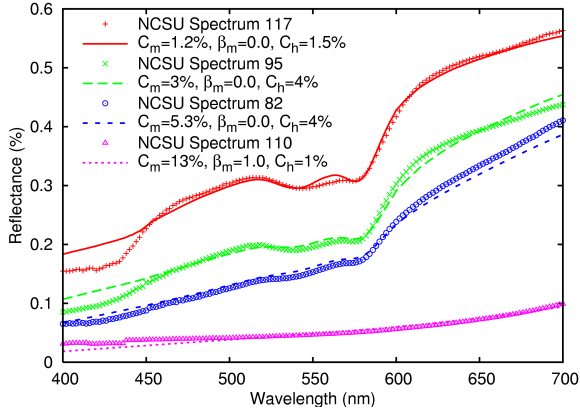

Figure 9: *Calculated total diffuse reflectance spectra compared to measured data from [VGI94]. From top to bottom, we compare with light Caucasian skin (spectrum number 117 in [VGI94]), dark Caucasian skin (spectrum 95), Asian skin (spectrum 82) and African-American skin (spectrum 110).*

adjusting the parameters. Figure 8 shows possible combinations of parameters to simulate different racial skin tones. On left side of the figure is light colored skin corresponding to Caucasian skin, while the right side image showing African skin has a much higher volume fraction of melanin. Both extremes have high concentrations of eumelanin. The middle image, corresponding to Asian skin, has a blend of eumelanin and pheomelanin. The far right image shows the effect of applying an albedo texture to the Caucasian skin; this increases the realism of the face as it adds variation as well as making the lips more reddish. The lower row of thin images are sections of photographs of real skin samples of the side of the face and neck from people of the corresponding ethnicities. These photographs were taken in a dark room under similar lighting conditions.

For a quantitative validation of our model, Figure 9 com-

pares generated total diffuse reflectance spectra to actual measured data from the NCSU spectral database [VGI94]. The spectra were calculated using Equation 9, completely decoupled from rendering. Note the simulated spectra capture the characteristic "W" shape in the middle of the visible spectrum due to the peaks in the hemoglobin absorption in the dermis, and the flattening of the spectra as melanin content increases. As shown in the figure, our model well approximates the shape of skin reflectance spectra, despite the simplicity of the model. The tradeoff for practicality is unfortunately a loss in precision, particulary below 450nm, but this does not seem to adversely affect the final color of skin during rendering. The parameters used are listed in the figure legend.

In Figure 10 we show different combinations of lighting and viewing directions on textured Caucasian skin (both pale and with a tan). The texture is an albedo texture map applied to the face using the technique in [DJ05].

6 Conclusions

We have presented a practical spectral shading model for human skin, that uses four physically based parameters to simulate a wide range of skin appearance including African, Asian and Caucasian skin. We model the skin as a two layer translucent material, accounting for spectral absorption and scattering within the layers, as well as surface reflectance. The four parameters to the model are total melanin content, melanin type, hemoglobin content, and surface oiliness.

In the future, we will investigate extending the model to handle abnormal concentrations of other chromophores, such as beta-carotene and bilirubin. Such extensions will make the model more complicated adding more terms to Equations 6 and 7, but would allow for modeling skin rashes or sunburns and other abornal skin conditions. It would also be useful to add asperity scattering [KP03] due to tiny hairs (peach fuzz) on the skin, or from an additional layer of cosmetics. Finally,

Figure 10: *Applying skin parameters to an entire face with texturing. The left image showing light pale Caucasian skin was generated with $C_m = 0.3\%$, $\beta_m = 0.25$, $C_h = 0.5\%$, and $\rho_s = 0.3$. The second image showing well-tanned Caucasian were generated with $C_m = 2\%$, $\beta_m = 0.25$, $C_h = 0.1\%$, and $\rho_s = 0.25$. The third images shows how our model captures the scattering of light through thin areas such as the ear, while the far right shows the skin illuminated from several directions. For both images, the parameters are $C_m = 0.2\%$, $\beta_m = 0.5$, $C_h = 1\%$, and $\rho_s = 0.25$.*

it would be interesting to use the model to automatically recover parameters from real skin.

7 Acknowledgments

References

[AAB*02] ALALUF S., ATKINS D., BARRETT K., BLOUNT M., CARTER N., HEATH A.: Ethnic variation in melanin content and composition in photoexposed and photoprotected skin. *Pigment Cell Res. 15* (2002), 112–118.

[AHC*01] ALALUF S., HEATH A., CARTER N., ATKINS D., MAHALINGAM H., BARRETT K., KOLB R., SMIT N.: Variation in melanin content and composition in Type V and VI photoexposed and photoprotected human skin: the dominant role of dhi. *Pigment Cell Res. 14* (2001), 337–347.

[AP81] ANDERSON R. R., PARRISH J. A.: The optics of human skin. *J. Invest. Dermatol. 77* (1981), 13–19.

[BGKT05] BASHKAOV A. N., GENINA E. A., KOCHUBEY V. I., TUCHIN V. V.: Optical properties of human skin, subcutaneous and mucous tissues in the wavelength range from 400 to 2000 nm. *J. Phys. D 38* (2005), 2543–2555.

[CT82] COOK R. L., TORRANCE K.: A reflectance model for computer graphics. In *ACM Trans. Graphic.* (1982), pp. 7–24.

[DHT*00] DEBEVEC P., HAWKINS T., TCHOU C., DUIKER H.-P., SAROKIN W., , SAGAR M.: Acquiring the reflectance field of a human face. In *Proceedings of ACM SIGGRAPH 2000* (New York, 2000), Computer Graphics Proceedings, ACM Press/Addison-Wesley Publishing Co., pp. 145–156.

[DJ05] DONNER C., JENSEN H. W.: Light diffusion in multi-layered translucent materials. *ACM Trans. Graphic. 24*, 3 (2005), 1032–1039.

[DJ06] DONNER C., JENSEN H. W.: Rapid simulation of steady-state spatially-resolved reflectance and transmittance profiles of multi-layered turbid materials. *J. Opt. Soc. Am. 23*, 6 (2006), 1382–1390.

[Her03] HERY C.: Implementing a skin bssrdf. *ACM SIGGRAPH 2003 Course 9* (2003), 73–88.

[HK93] HANRAHAN P., KRUEGER W.: Reflection from layered surfaces due to subsurface scattering. In *Proceedings of ACM SIGGRAPH 1999* (New York, 1993), Computer Graphics Proceedings, ACM Press/Addison-Wesley Publishing Co., pp. 164–174.

[HOD*05] HENNESSY A., OH C., DIFFEY B., WAKAMATSU K., ITO S., REES J.: Eumelanin and pheomelanin concentrations in human epidermis before and after UVB radiation. *Pigment Cell Res. 18* (2005), 220–223.

[INN05] IGARASHI T., NISHINO K., NAYAR S. K.: *The Appearance of Human Skin*. Technical Report CUCS-024-05, Columbia University, 2005.

[IW06] ITO S., WAKAMATSU K.: Quantitative analysis of

eumelanin and pheomelanin in humans, mice, and other animals: a comparative review. *Pigment Cell Res. 16* (2006), 523–531.

[Jac96] JACQUES S. L.: Origins of tissue optical properties in the uva, visible, and nir regions. In *OSA TOPS on Advances in Optical Imaging and Photon Migration* (1996), vol. 2, pp. 364–371.

[Jac98] JACQUES S. L.: Skin optics. *Oregon Medical Laser Center News* (1998), http://omlc.ogi.edu/news/jan98/skinoptics.html.

[JB02] JENSEN H. W., BUHLER J.: A rapid hierarchical rendering technique for translucent materials. *ACM Trans. Graphic. 21* (2002), 576–581.

[JM91] JACQUES S. L., MCAULIFFE D. J.: The melanosome: threshold temperature for explosive vaporization and internal absorption coefficient during pulsed laser irradiation. *Photochem. Photobiol. 53* (1991), 769–775.

[JMLH01] JENSEN H. W., MARSCHNER S. R., LEVOY M., HANRAHAN P.: A practical model for subsurface light transport. In *Proceedings of ACM SIGGRAPH 2001* (New York, 2001), Computer Graphics Proceedings, ACM Press/Addison-Wesley Publishing Co., pp. 511–518.

[KB04] KRISHNASWAMY A., BARANOSKI G. V. G.: A biophysically-based spectral model of light interaction with human skin. In *Proceedings of EUROGRAPHICS 2004* (2004), vol. 23.

[KP03] KOENDERINK J., PONT S.: The secret of velvety skin. *Mach. Vision Appl. 14*, 4 (2003), 260–268.

[MM02] MEGLINSKI I. V., MATCHER S. J.: Quantitative assessment of skin layers absorption and skin reflectance spectra simulation in the visible and near-infrared spectal regions. *Physiol. Meas. 23* (2002), 741–753.

[MWL*99] MARSCHNER S. R., WESTIN S. H., LAFORTUNE E. P. F., TORRANCE K. E., GREENBERG D. P.: Image-based BRDF measurement including human skin. In *Rendering Techniques '99 (Proceedings of the 10th Eurographics Rendering Workshop)* (1999), pp. 119–130.

[NL01] NG C. S.-L., LI L.: A multi-layered reflection of natural human skin. In *Computer Graphics International 2001 (CGI'01)* (2001), pp. 249–266.

[SJT95] SAIDI I. S., JACQUES S. L., TITTEL F. K.: Mie and Rayleigh modeling of visible-light scattering in neonatel skin. *Appl. Opt. 34*, 31 (1995), 7410–7418.

[SMPW03] SANDBY-MOLLER J., POULSEN T., WULF H. C.: Influence of epidermal thickness, pigmentation and redness on skin autofluorescence. *Photochem. Photobiol. 77*, 6 (2003), 616–620.

[SS98] SARNA T., SWARTZ H. M.: The physical properties of melanins. In *The Pigmentary System: Physiology and Pathophysiology*, Nordlund J. J., Boissy R. E., Hearing V. J., King R. A.,, Paul Ortonne J., (Eds.). Oxford University Press, 1998, ch. 25, pp. 333–357.

[SSAS97] SPOTT T., SVAASAND L. O., ANDERSON R. E., SCHMEDLING P. F.: Application of optical diffusion theory to transcutaneous bilirubinometry. In *Proc. SPIE* (1997), vol. 3195, pp. 234–245.

[Sta01] STAM J.: An illumination model for a skin layer bounded by rough surfaces. In *Proceedings of the 12th Eurographics Workshop on Rendering* (2001), pp. 39–52.

[SzZKB04] STAMATAS G. N., Z. ZMUDZKA B., KOLLIAS N., BEER J. Z.: Non-invasive measurements of skin pigmentation in situ. *Pigment Cell Res. 17* (2004), 618–626.

[TG79] TAKATANIA S., GRAHAM M. D.: Theoretical analysis of diffuse reflectance from a two-layer tissue model. *IEEE Trans. Biomed. Eng. 26*, 12 (1979), 656–664.

[TM99] TSUMURA N., MIYAKE Y.: Independent component analysis of skin color image. *J. Opt. Soc. Am. 16*, 9 (1999), 2169–2176.

[TOS*03] TSUMURA N., OJIMA N., SATO K., SHIRAISHI M., SHIMIZU H., NABESHIMA H., AKAZAKI S., HORI K., MIYAKE Y.: Image-based skin color and texture analysissynthesis by extracting hemoglobin and melanin information in the skin. *ACM Trans. Graphic. 22*, 3 (2003), 770–779.

[TS67] TORRANCE K., SPARROW E.: Theory for off-specular reflection from roughened surfaces. *J. Opt. Soc. Am. 57* (1967), 1104–1114.

[VGI94] VRHEL M. J., GERSHON R., IWAN L. S.: Measurement and analysis of object reflectance spectra. *Color Res Appl. 19*, 1 (1994), 2–9.

[vJSS89] VAN GEMERT M. J. C., JACQUES S. L., STERENBORG H. J. C. M., STAR W. M.: Skin Optics. *IEEE Trans. Biomed. Eng. 36* (1989), 1146–1154.

[WKK*06] WAKAMATSU K., KAVANAGH R., KADEKARO A. L., TERZIEVA S., STURM R. A., LEACHMAN S., ABDEL-MALEK Z., ITO S.: Diversity of pigmentation in cultured human melanocytes is due to differences in the type as well as quantity of melanin. *Pigment Cell Res. 19* (2006), 154–162.

[WMP*06] WEYRICH T., MATUSIK W., PFISTER H., BICKEL B., DONNER C., TU C., MCANDLESS J., LEE J., NGAN A., JENSEN H. W., GROSS M.: Analysis of human faces using a measurement-based skin reflectance model. *ACM Trans. Graphic. 25* (2006), to appear.

[ZBK01] ZONIOS G., BYKOWSKI J., KOLLIAS N.: Skin melanin, hemoglobin, and light scattering properties can be quantitatively assessed *In Vivo* using diffuse reflectance spectroscopy. *J. Comput. Phys. 81* (2001), 137–150.
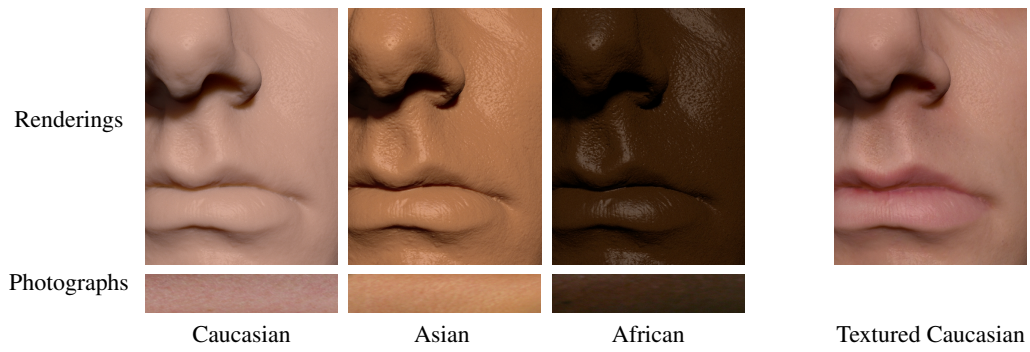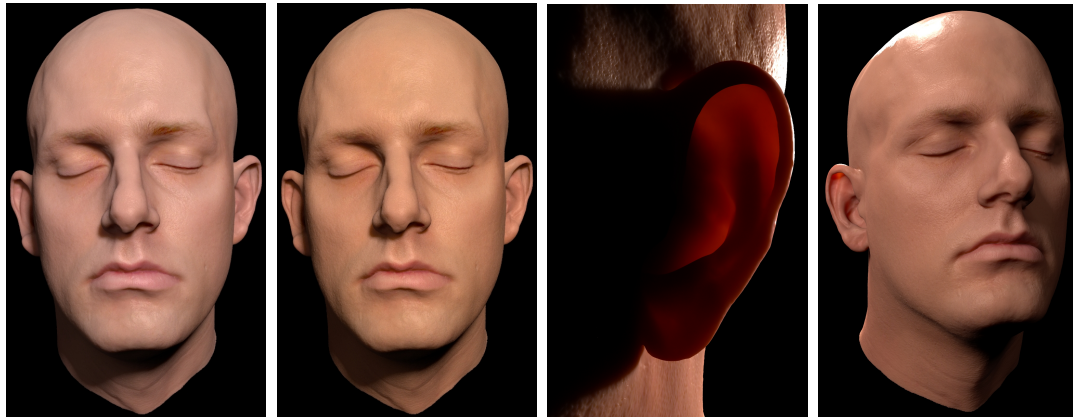
Renderings

Photographs

| Caucasian | Asian | African | Textured Caucasian |

Figure 8: *Color plate.*

Figure 10: *Color plate.*